energy&fuels

pubs.acs.org/EF

Article

Breakthrough Zn(II) Catalyst for Direct Air Capture Employing CO_2 Hydration

Published as part of Energy & Fuels special issue "Recent Advances in Carbon Capture, Utilization, and Sequestration (CCUS)".

Priyabrata Biswal, Moushumi Sarma, Xin Gao, Saloni Bhatnagar, Sean R. Parkin, Kunlei Liu, and Jesse Thompson*

Cite This: *Energy Fuels* 2026, 40, 5221−5232

Read Online

ACCESS | Metrics & More | Article Recommendations | Supporting Information

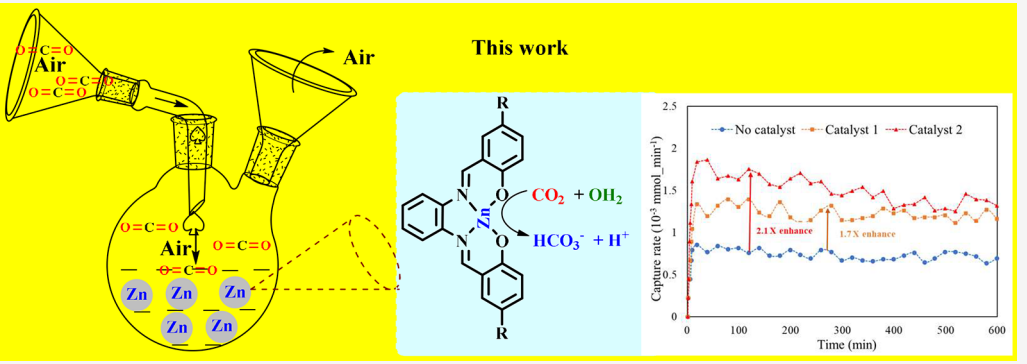

ABSTRACT: Direct air capture (DAC) represents a vital technology for atmospheric CO_2 remediation, but few studies have tested catalysts at dilute atmospheric CO_2 concentrations. Inspired by the carbonic anhydrase metalloenzyme, we report a catalytic DAC strategy employing robust zinc(II) enzyme mimics that enable efficient CO_2 sequestration pathways. A catalyst-mediated CO_2 hydration cycle in aqueous sorbents facilitates accelerated capture from dilute atmospheric air, thereby addressing the kinetic limitations observed in carbonate-based systems. Our developed complexes [ZnC1] and [ZnC2] enhance capture rates up to 2-fold at millimolar concentrations and improve the CO_2 mass transfer by 40−60% in 1 M K_2CO_3 sorbent under ambient conditions. These bench-stable, earth-abundant zinc catalysts operate effectively under dilute CO_2 concentrations, overcoming the kinetic limitations of conventional carbonate-based sorbents. Mechanistic studies support a biomimetic catalytic cycle that facilitates rapid CO_2 conversion, demonstrating that a catalyst-assisted DAC can enable energy-efficient, scalable carbon capture technologies.

INTRODUCTION

Atmospheric carbon dioxide (CO_2) concentrations have increased from preindustrial levels of approximately 280 ppm to around 430 ppm in 2025 primarily due to anthropogenic activities. The rapid increase in atmospheric CO_2 concentration is a major driver of global climate change, contributing to global temperature rise, ocean acidification, sea level rise, altered precipitation patterns, and widespread ecological disruption.[1−4] These environmental impacts present significant challenges for both natural ecosystems and human societies,[1,2,5] underscoring the urgent need for effective and sustainable negative-emission technologies (NETs) to mitigate CO_2 accumulation.[6,7] Among the emerging NETs, direct air capture (DAC) has emerged as a promising NET for reducing atmospheric CO_2 accumulation.[8−11] Unlike conventional carbon capture systems, which target concentrated emission streams (10−20% CO_2) at point sources (steel plants and industrial facilities),[12−16] DAC removes CO_2 from ambient air (~430 ppm).[8−11]

This approach offers unique advantages in mitigating both hard-to-abate emissions and CO_2 accumulated in the atmosphere.[17,18] Current DAC technologies are primarily based on liquid sorbent systems, employing aqueous hydroxides and alkanolamines, or solid sorbent systems, utilizing materials such as metal−organic frameworks (MOFs), zeolites, and amine-functionalized polymers.[19−22] Several large-scale DAC facilities are now operational or under

Received: December 2, 2025
Revised: February 19, 2026
Accepted: February 20, 2026
Published: March 2, 2026

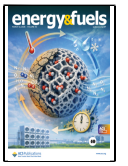

ACS Publications

© 2026 The Authors. Published by American Chemical Society

construction, including projects in Iceland (36 kt of CO_2/year, operational 2024) and the United States (500 kt of CO_2/year, operational 2025).

However, the fundamental challenge with DAC is the extremely low concentration of atmospheric CO_2 (~430 ppm) compared to point-source systems, which creates severe kinetic constraints.[23−25] In alkaline DAC systems, these kinetic limitations appear clearly despite thermodynamically favorable CO_2 absorption; the process exhibits sluggish absorption kinetics due to slow gas−liquid mass transfer.[26−30] Such kinetic limitations translate into severe technical and economic barriers for large-scale DAC deployment. Current systems require high regeneration energy (>100 °C, 150−200 kJ/mol CO_2)[26] and suffer from significant capacity degradation (20−30% loss over 100 cycles)[31,32] and capture costs of $400−1,000 per ton CO_2,[33−35] far exceeding the ~$100 per ton threshold for economic viability. Moreover, the energy requirements for sorbent regeneration alone accounts for 60−80% of total operating costs.[19,20,34,36] The International Energy Agency projects that achieving 7.6 Gt CO_2 removal annually by 2050 with existing DAC technologies could consume 10−20% of global electricity production,[18,37] underscoring the urgent need for advances in catalyst design to improve reaction kinetics.

Nature offers a highly efficient solution for CO_2 capture through carbonic anhydrase (CA), a metalloenzyme that accelerates CO_2 hydration up to 10^6-fold.[38,39] At its active site, CA features a tetrahedral zinc(II) active site, coordinated by three histidine residues, catalyzing CO_2 hydration via sequential water activation followed by zinc-OH nucleophilic attack.[38,40,41] This exceptional catalytic efficiency inspires researchers to develop biomimetic catalysts. Early complexes such as $[Zn(cyclen)(H_2O)][ClO_4]_2$ established key design principles,[42−53] including (a) tetradentate ligand frameworks for enhanced stability in aqueous solvents, (b) superior catalytic efficiency of zinc(II) over cobalt(III) due to enhanced Lewis acidity, and (c) the critical role of the secondary coordination sphere.[45,46,54−56] Biomimetic catalysts based on these principles have demonstrated substantial improvements in point-source carbon capture, achieving 40−60% enhancements in CO_2 absorption rates.[45,50,51] Recent advances further highlight the importance of secondary coordination sphere modifications, such as incorporating additional hydrogen bonding sites, which significantly enhance catalytic performance in the CO_2 hydration reaction ($H_2O + CO_2 \rightarrow H^+ + HCO_3^-$).[42,45,47,50,51]

Although catalysts have shown strong promise in point-source CO_2 capture, their use in direct air capture at low atmospheric concentrations has still been largely unexplored. This represents a fundamental gap in DAC technology development and motivates the present study. While biomimetic catalysts have proven effective in concentrated CO_2 streams (10−20%),[42,45,47,50,51] no systematic study has evaluated catalyst performance under the extreme kinetic constraints imposed by atmospheric conditions (~430 ppm). The questions of whether molecular catalysts can overcome these barriers in practical DAC systems and how catalyst design principles must be adapted for dilute atmospheric capture remain unanswered. Moreover, catalyst integration with economically viable sorbent systems, particularly carbonate-based media that offer lower regeneration energies (1.5−2.5 GJ/t CO_2) compared to amine systems (3.5−4.5 GJ/t CO_2), has not been systematically investigated.[34,57−61]

The implementation of catalyst-assisted DAC must also consider system integration and regeneration strategies. In aqueous alkaline DAC systems, captured CO_2 reacts with KOH to form potassium carbonate (K_2CO_3) and bicarbonate ($KHCO_3$) species, requiring continuous hydroxide regeneration through closed-loop processes.[19,29,62,63] The conventional lime loop involves causticization of K_2CO_3 with $Ca(OH)_2$, producing KOH and $CaCO_3$, with calcination of $CaCO_3$ at ~900 °C, releasing high-purity CO_2.[64−67] Our group has demonstrated electrochemical regeneration of hydroxide from carbonate/bicarbonate solutions using bipolar membrane electrodialysis (BMED), which produces alkaline hydroxide solutions and concentrated CO_2 streams while avoiding high-temperature calcination.[63] Integration of biomimetic catalysts with BMED regeneration systems represents a promising direction for closed-loop DAC operation. However, Schiff-based ligands are susceptible to hydrolysis under acidic conditions. For practical BMED integration, catalyst separation before the electrochemical regeneration step or development of heterogeneous immobilized catalysts with enhanced pH stability will be necessary for closed-loop operation. Foaming in liquid sorbent systems can reduce mass transfer efficiency, cause equipment fouling, and lead to sorbent carryover.[50,68−70] Traditional antifoam additives used to reduce the foaming behavior may interfere with the catalyst performance and require separate recovery systems. Therefore, developing catalysts that minimize foaming while maintaining high activity represents another critical design consideration for economically viable DAC technology.

To address this critical technological gap, we report the first systematic study of catalyst-assisted DAC, introducing a series of zinc(II) enzyme mimics specifically engineered for operation in aqueous carbonate media under ambient atmospheric conditions. Building upon our previous work developing biomimetic catalysts for amine-based solvents,[50,71,72] our design strategy emphasizes secondary coordination sphere modifications that promote CO_2 hydration through strategic hydrogen bonding and polar interactions. The developed complexes [ZnC1] and [ZnC2] exhibit 2-fold enhancement in capture rates at millimolar catalyst concentrations, 50% improvement in absorption efficiency with 1 M K_2CO_3 sorbent, and 40−60% augmentation in CO_2 mass transfer under ambient conditions. These bench-stable, earth-abundant zinc catalysts operate under mild conditions and function at dilute atmospheric CO_2 concentrations. The enzyme-mimetic mechanism provides a molecular framework for understanding the enhanced capture kinetics. This preliminary study establishes fundamental structure−activity relationships and catalytic mechanisms that provide a foundation for next-generation heterogeneous catalyst systems compatible with electrochemical regeneration pathways for practical DAC deployment. Mechanistic investigations support a biomimetic catalytic cycle that circumvents the sluggish kinetics of conventional carbonate systems. This work establishes catalyst-assisted DAC as a viable strategy for atmospheric CO_2 reduction and provides a foundation for next-generation carbon capture technologies that bridge the performance gap between thermodynamically favorable carbonate systems and kinetically superior amine systems.

https://doi.org/10.1021/acs.energyfuels.5c06296
Energy Fuels 2026, 40, 5221−5232

EXPERIMENTAL SECTION

Catalyst Synthesis

For catalyst employment in large-scale commercial DAC applications, the ease of synthesis, purification efficiency, and synthesis cost represent critical components. The synthetic route must be amenable to multikilogram scale production while maintaining high purity standards. The raw material costs approximately 15−20% of the total catalyst production cost, with synthesis and purification contributing an additional 25−30%. The developed complexes are synthesized via four streamlined synthetic steps (see the Supporting Information), wherein the desired products are obtained as solids by simple precipitation or recrystallization, which can be collected by filtration without requiring chromatographic purification or extensive workup procedures. This simplified approach minimizes waste generation and reduces the synthesis time, making the catalysts economically viable for large-scale applications. We synthesized the precursor 2-hydroxy-5-chloromethyl-benzaldehyde and its morpholine derivative 2-hydroxy-5-(morpholino methyl)benzaldehyde according to the literature procedures. The corresponding salen ligands (L1 and L2) and their zinc(II) complexes ZnC1 and ZnC2 were prepared via Schiff base condensation and subsequent metalation following adapted literature methods.[50]

CO_2 Capture Evaluation

Catalyst performance under DAC conditions was assessed using a pH drop monitoring technique adapted from established methods.[45,73] The experimental setup consists of a 30 mL gas−water saturator, a single mass flow controller, a glass impinger, a pH probe, and a three-neck round-bottom flask containing 25 mL of capture solution (Figure 1). Both the saturator and impinger are made of Pyrex. A compressed air stream containing ∼430 ppm of CO_2 was saturated in the water-filled saturator (20 mL) and bubbled at a controlled flow rate of 0.5 L/min into the capture solution. The pH probe goes through the other neck of the round-bottom flask to record the continuous pH changes over time. The rate of pH decrease is directly related to CO_2 absorption kinetics, providing a quick screening method for catalyst performance evaluation under standard conditions.

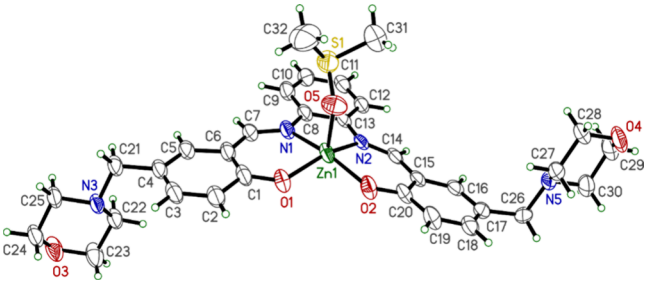

Figure 1. X-ray crystal structure of the ZnC1 complex.

Quantitative CO_2 capture rates and loading capacities were measured using breakthrough analysis.[4,45] The setup includes a 30 mL Pyrex gas saturator, a single mass flow controller, a glass impinger, a three-necked round-bottom flask with 25 mL of capture solution, two condensers for moisture removal, and a nondispersive infrared CO_2 analyzer (GM-70, Vaisala) (Figure 1). A compressed air stream containing ∼430 ppm of CO_2 was saturated in the water-filled saturator (20 mL) and bubbled through the capture solution. The effluent gas was condensed using the condenser, dried with drierite to remove moisture, and then passed through the analyzer for continuous CO_2 concentration data collection at 1 min intervals. The difference between inlet and outlet CO_2 concentrations indicates the immediate CO_2 capture at a specific moment, and integrating this concentration difference over time provides the CO_2 capture rate as shown in eq 1.

$$\text{CO2 capture rate(mol } CO_2\text{/min)} = \frac{\int_0^t (C_{in} - C_{out}(t))}{dt} \quad (1)$$

in which C_{in} is the initial CO_2 concentration in mol, C_{out} is the CO_2 effluent concentration in mol at that time, and t is the time in minutes. The breakthrough method provides a more precise analysis compared to the pH drop technique, providing the capture rates and total CO_2 loading capacity. The continuous monitoring enables the detection of saturation behavior and the assessment of catalyst stability over extended operating periods.

Foam formation during gas−liquid contact is a significant operational concern for liquid-phase DAC systems, as excessive foaming can reduce volumetric mass transfer coefficients, result in equipment fouling, and cause sorbent carryover losses.[69,70,74] The foaming behavior was systematically examined to evaluate the effect of gas-bubble interactions on the overall mass transfer efficiency and the catalyst efficiency. The experiments were carried out in a 1 L cylindrical volumetric flask using a sintered glass diffuser (60 μm nominal pore size). A compressed air stream containing ∼430 ppm of CO_2 was saturated in the water-filled saturator (20 mL) and bubbled at a controlled flow rate of 0.5 L/min into 100 mL of 1 M K_2CO_3 solution, both with and without catalyst (0.03 mmol of catalyst). The scale marked on the volumetric flask was used to measure the foam height, $H(t)$, over time.

RESULTS AND DISCUSSION

Rational Catalyst Design and Synthesis

Carbonic anhydrase (CA) is widely recognized for its extraordinary ability to accelerate the hydration of CO_2 into bicarbonate. This remarkable activity of CA is attributed to the finely tuned coordination environment surrounding its Zn(II) center, supported by secondary interactions that facilitate proton transfer and substrate orientation with precision. Inspired by the structural feature of this natural enzyme, we set out to design and synthesize a series of Zn(II) complexes supported by salen-based ligands, to mimic the key geometries of CA, and to evaluate their efficacy in catalyst-assisted DAC via CO_2 hydration.

Salen ligands have several advantages for designing biomimetic catalysts due to their easy synthesis, tunable electronic properties, and flexible coordination geometries around metal centers. They offer tetradentate chelation, enhancing complex stability compared to monodentate or bidentate alternatives and providing a critical structural stability for operation in an aqueous medium under ambient conditions. Considering the versatility and robustness of salen ligands, we synthesized morpholine-based salen ligands to enhance secondary sphere interactions. We chose the morpholine group for its ability to form hydrogen bonding networks as well as its basic nitrogen center, which can participate in proton relay mechanisms, mimicking the CA active site. In biomimetic catalytic systems, tertiary amines may serve as secondary-sphere proton-transfer mediators rather than direct CO_2 hydration catalysts, similar to histidine residues in carbonic anhydrase.[38,39,54−56] The catalytic hydration mechanism requires two essential structural features: (1) a Lewis-acidic metal center (Zn^{2+}) that activates CO_2 and (2) a metal-bound hydroxide nucleophile (Zn-OH) that attacks the electrophilic carbon. Meanwhile, free tertiary amines can promote CO_2 absorption via base-catalyzed proton acceptance at molar concentrations (2.5−5.0 M) used in industrial amine scrubbing for flue gas.[75,76]

We synthesized two Zn(II) complexes (ZnC1 and ZnC2) via Schiff base condensation between *o*-phenylenediamine or

https://doi.org/10.1021/acs.energyfuels.5c06296
Energy Fuels 2026, 40, 5221−5232

Scheme 1. Synthesis of the Zinc(II) Complex

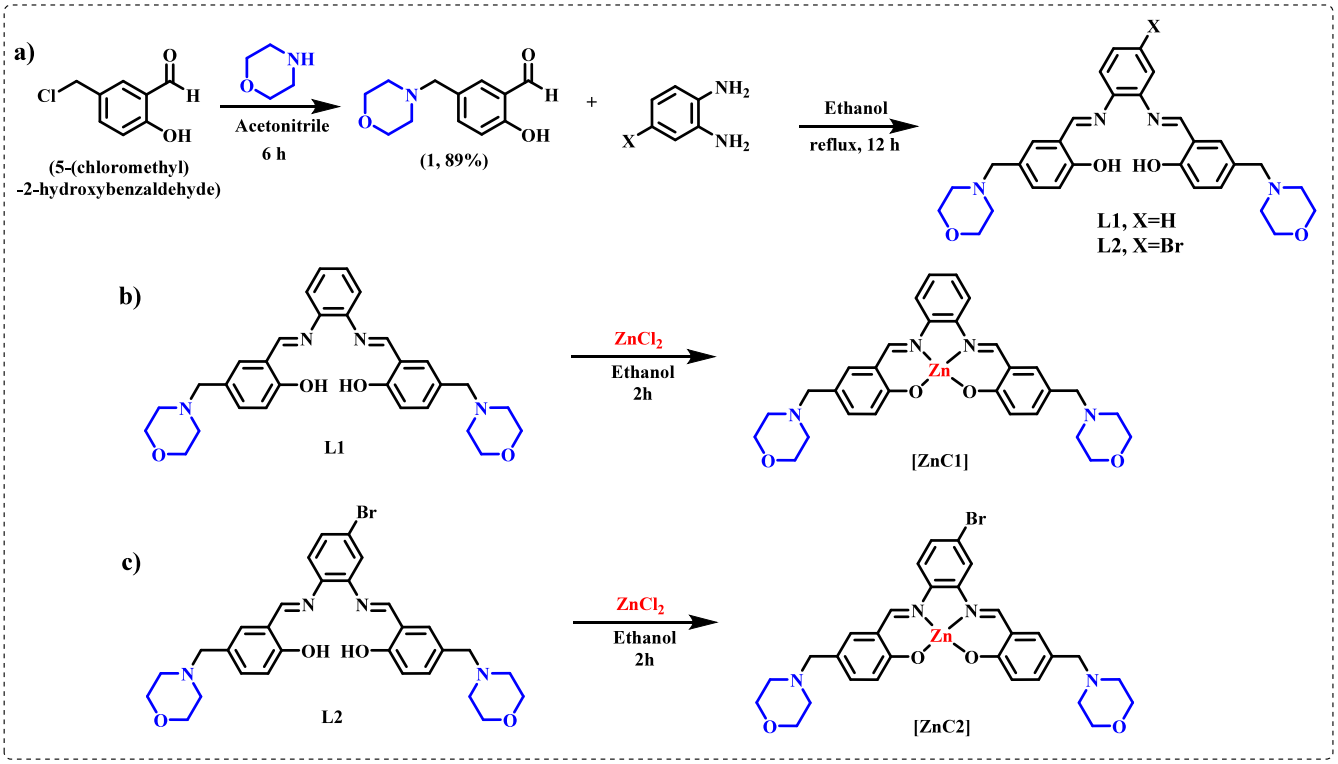

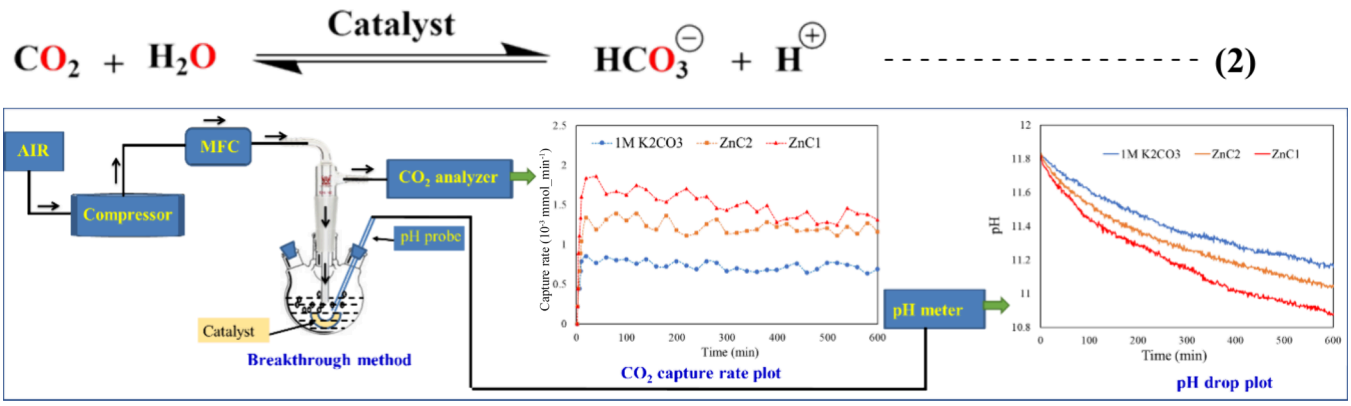

Figure 2. Laboratory testing of our catalyst for CO_2 hydration and the corresponding data plots.

4-bromo-*o*-phenylenediamine with 5-(morpholinomethyl)-salicylaldehyde. Then, we metalated these Schiff base ligands with $ZnCl_2/Zn(OAc)_2{\cdot}2H_2O$ under reflux in ethanol (Scheme 1). The complexes ZnC1 and ZnC2 contain salen-type ligands that have phenyl and bromophenyl frameworks, respectively. We obtained both complexes as air-stable solids with yields >95%, and their complexation was confirmed by ^1H NMR spectroscopy. Mass spectrometry analysis confirms the mononuclear nature of the complexes, showing molecular ion peaks that match the suggested structures. UV−vis spectroscopy showed characteristic ligand-to-metal charge transfer bands in the 350−450 nm range, further confirming the complexation. Both complexes dissolve well in polar organic solvents and demonstrate remarkable thermal and oxidative stability, which is essential for catalytic direct air capture applications in aqueous media.

To our delight, we observed the single crystal of the ZnC1 catalyst, and it crystallized in a monoclinic system with space group *C*2/*c*. Single-crystal X-ray diffraction analysis reveals a distorted square planar geometry for ZnC1 around the Zn(II) center coordinated by two imine nitrogen and two phenolic oxygen donors from the tetradentate salen ligand. The four-coordinate geometry index $\tau_4 = 0.32$ (calculated as $\tau_4 = [360° - (\alpha + \beta)]/141°$, where α and β are the two largest L−Zn−L angles) confirms geometry closer to square-planar ($\tau_4 = 0$) than tetrahedral ($\tau_4 = 1$), with the Zn−N and Zn−O bond distances (1.97−2.05 Å) comparable to other salen-Zn(II) complexes. Full crystallographic parameters are provided in Table S3 (Supporting Information).

The ZnC1 complex has a phenyl backbone that maintains ligand geometry more symmetric and planar and promotes efficient orbital overlap. In the case of the ZnC2 complex, we are unable to isolate a single crystal, whereas from ^1H NMR analysis, we observe steric distortion in the ZnC2 complex, having distinct sets of protons. The bromo substituent causes steric distortion in the ligand framework, which in turn can

https://doi.org/10.1021/acs.energyfuels.5c06296
Energy Fuels 2026, 40, 5221−5232

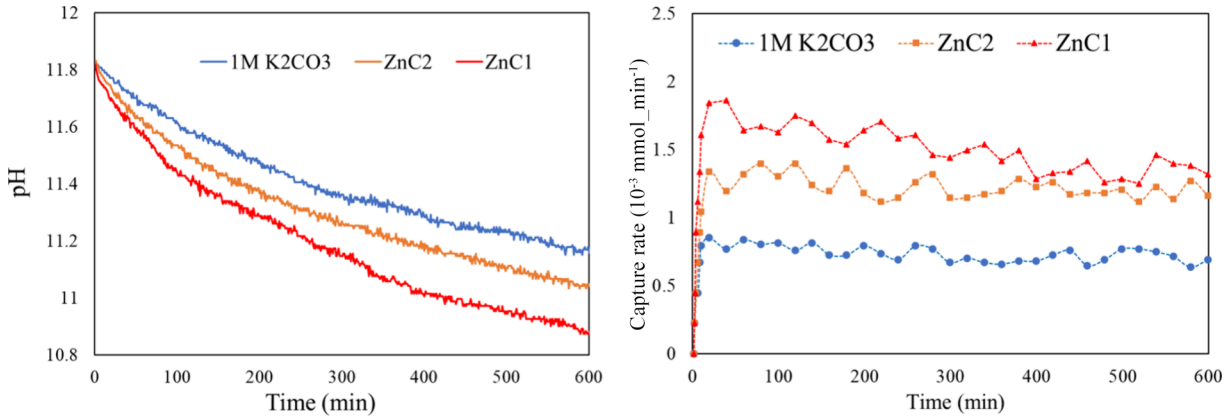

Figure 3. (Left) pH drop testing of complexes ZnC1 and ZnC2 in 1 M K_2CO_3 solution and blank 1 M K_2CO_3 solution. (Right) Carbon capture rate of ZnC1 and ZnC2 in 1 M K_2CO_3 solution and blank 1 M K_2CO_3 solution.

hinder the orbital overlap efficiency and affect the catalytic efficiency. The electron-withdrawing nature of the bromine is further reflected in the downfield shifts of the ^{1}H NMR signals for protons adjacent to the metal coordination sphere. The combination of structural stability, electronic properties, and secondary sphere functionalization makes these complexes promising candidates for catalyst-assisted direct air capture.

Catalytic Evaluation for CO_2 Capture

We systematically tested Zn(II) complexes ZnC1 and ZnC2 to evaluate their catalytic efficiency in enhancing CO_2 mass transfer in aqueous potassium carbonate solution under direct air capture (DAC) conditions. We designed a small-scale testing apparatus with a round-bottom flask containing the catalyst and liquid sorbent (25 mL of 1 M aqueous K_2CO_3). A compressed air stream containing ∼430 ppm of CO_2 was saturated in the water-filled saturator (20 mL) and bubbled at a controlled flow rate of 0.5 L/min (Figure 2). We used two different methods to measure the catalyst performance: the pH drop method, which is a quick screening method to check how many protons are released during the catalytic hydration of CO_2 to bicarbonate, and the breakthrough solvent evaluation method, which gives us a precise CO_2 capture rate.

We conducted initial baseline measurements without a catalyst to evaluate the CO_2 absorption capacity of the 1 M K_2CO_3 sorbent, providing a reference for assessing the catalytic enhancement. The uncatalyzed system captured only about 20% of the CO_2 from air, corresponding to a rate of 0.72 μmol of CO_2 per minute. This low capture efficiency highlights the kinetic limitations of the uncatalyzed DAC system using a 1 M K_2CO_3 sorbent at low atmospheric concentrations (∼430 ppm). In contrast, after the addition of ZnC1 and ZnC2 complexes, we observed a promising enhancement in CO_2 mass transfer within 5 to 10 min, highlighting their catalytic efficiency in the CO_2 hydration reaction under DAC conditions. We evaluated the catalytic efficiency of ZnC1 and ZnC2 using the pH drop method to monitor proton release (eq 2) during CO_2 hydration into bicarbonate.[45] This method helps in quick comparison of different catalysts with variable concentrations. In the absence of a catalyst, the pH slowly dropped to pH 11.3 over the course of 600 min, indicating that the CO_2 hydration in carbonate solutions at DAC conditions is naturally slow. In contrast, the addition of ZnC1 (17 mg, corresponding to 0.030 mmol) dramatically accelerated the pH drop, with the solution reaching pH 11.3 in 200 min, representing a huge improvement in reaction rate. Similarly, the catalyst ZnC2 (20 mg or 0.030 mmol) also showed similar catalytic activity, reaching pH 11.3 in 300 min (Figure 3, left).

Control experiments using ligand-only and metal salt ($ZnCl_2$)-only systems showed no measurable rate enhancement relative to the uncatalyzed baseline (Figures S4 and S5, Supporting Information), confirming that the observed catalytic activity requires both the salen ligand framework and Zn(II) coordination. This is consistent with literature reports showing that Schiff-base ligands require metal coordination for CO_2 hydration activity.[4,50,72] Throughout the 600 min testing period, both ZnC1 and ZnC2 showed steady activity with no sign of catalyst deactivation, ligand dissociation, or metal leaching.

To measure the capture rate enhancement in the presence of ZnC1 and ZnC2 under DAC conditions, we performed a series of breakthrough capture analyses using CO_2 concentration monitoring data. The uncatalyzed system captured only about 20% of the CO_2 from air, corresponding to a rate of 0.72 μmol CO_2/min, whereas after the addition of ZnC1 catalyst, the capture rate doubled, reaching up to 1.5 μmol CO_2/min, while ZnC2 reached 1.2 μmol CO_2/min (Figure 3, right). ZnC1 and ZnC2 clearly enhanced the CO_2 hydration reaction under the DAC conditions. The catalytic enhancement of 2.1-fold in the case of the ZnC1 catalyst and 1.7-fold for the ZnC2 catalyst represents a critical parameter for the large-scale DAC applications.[50,72,77] The better performance of ZnC1 is due to its more planar ligand geometry, which enables better orbital overlapping, better substrate interactions, electron delocalization, and ligand field stabilization. This can improve electron delocalization between the ligand and the metal center, making the metal center more active. On the other hand, the bromine substituent in ZnC2 causes small geometric distortions in the ligand framework, hindering the orbital overlap and electron delocalization and, as a result, minimizing the reactivity of the metal complex. All of these factors make ZnC1 a better catalyst and increase its activity for the CO_2 hydration reaction under DAC conditions.

A comprehensive analysis of total mass transfer[50,72] further confirms the catalyst-assisted enhancement observed under DAC conditions (Figure 4). The time-dependent CO_2 capture profiles showed that the catalyzed systems not only exhibit faster initial rates but also achieve higher total loading capacities. The total mass transfer coefficients were calculated according to

https://doi.org/10.1021/acs.energyfuels.5c06296
Energy Fuels 2026, 40, 5221−5232

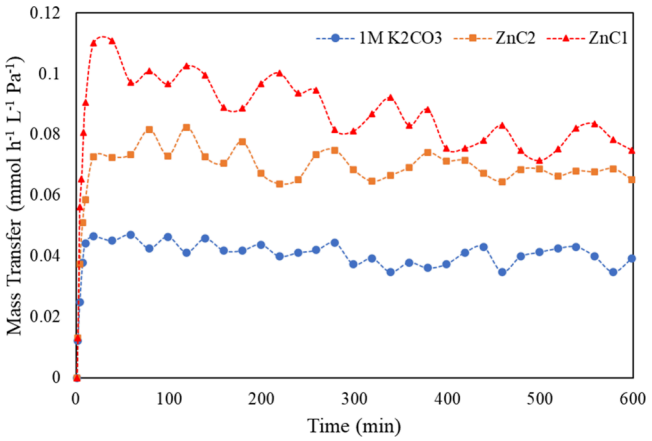

Figure 4. Mass transfer in the presence of complexes ZnC1 and ZnC2 in 1 M K_2CO_3 solution.

$$\text{mass transfer}\left(\frac{\text{mol}}{\text{h}\cdot\text{L}\cdot\text{Pa}}\right) = \frac{\text{CO}_2\text{ flow rate}\left(\frac{\text{mol}}{\text{h}}\right)}{\text{partial pressure of CO}_2\text{(Pa)}}$$

$$\text{CO}_2\text{ flow rate}\left(\frac{\text{mol}}{\text{h}}\right) = \frac{\%\text{ of CO}_2}{100} \times \text{CO}_2\text{ flow rate}\left(\frac{\text{L}}{\text{min}}\right) \times \frac{60}{22.4}$$

$$\text{partial pressure of CO}_2\text{(Pa)} = \frac{\frac{p_1 \times 101{,}325}{10^6} - \frac{p_2 \times 101{,}325}{10^6}}{\ln\left(\frac{p_1 \times 101{,}325}{10^6}\right) - \ln\left(\frac{p_2 \times 101{,}325}{10^6}\right)}$$

The total mass transfer data demonstrate that the presence of ZnC1 and ZnC2 catalysts significantly enhances the total mass transfer compared with the catalyst-free 1 M K_2CO_3 system under similar conditions. Further, the total CO_2 loading capacity measurements (Table 1) highlighted higher CO_2 loadings of 0.200 and 0.121 mol/kg in the presence of ZnC1 and ZnC2 compared to only 0.023 mol/kg without a catalyst, representing 8.7- and 5.3-fold improvements, respectively. These findings highlight the strong catalytic effect of both complexes in facilitating CO_2 absorption under DAC conditions, with ZnC1 outperforming ZnC2 due to its favorable structural features.

Table 1. Physical Properties of the Solvent in the Presence of ZnC1 and ZnC2 Catalysts

sample	density (g/mL)	CO_2 loading (mol/kg)	additional CO_2 loading (mol/kg)
1 M K_2CO_3	1.119	1.03	
loaded 1 M K_2CO_3	1.123	1.05	0.023
Zn-C1	1.118	0.99	
loaded Zn-C1	1.125	1.20	0.2
Zn-C2	1.118	1.01	
loaded Zn-C2	1.126	1.13	0.121

Concentration-Dependent Catalytic Activity

To elucidate the relationship between catalyst concentration and capture rate,[78] we conducted systematic kinetic experiments using different ZnC1 and ZnC2 loadings from 5 to 50 mg (corresponding to 0.008−0.08 mmol catalyst concentrations) (Table 2, Figure S2 and S3 in Supporting Information). The concentration dependence capture rate analysis is crucial for optimizing the catalyst loading and identifying the minimum effective catalyst concentration that ensures economic viability. For both ZnC1 and ZnC2, capture rates increased similarly with an increase in catalyst concentration from 0.008 to 0.030 mmol, indicating first-order kinetics with respect to catalyst concentration in this range. It reflects that the catalyst aggregation or deactivation is negligible at low to moderate concentrations, with each molecule catalyzing the reaction. The ZnC1 catalyst reached its maximum capture rate of 1.51 μmol/min at 0.030 mmol, while ZnC2 achieved 1.23 μmol/min at the same loading. Beyond this point, we observed no significant improvement even at higher concentrations (up to 0.080 mmol), reflecting the saturation behavior. This saturation indicates that once the gas−liquid interface is sufficiently populated with catalytic sites, further increases in bulk catalyst concentration do not accelerate interfacial reaction kinetics. Instead, the rate-limiting step shifts from the availability of catalytically active sites to the mass transfer of CO_2 across the gas−liquid boundary. Similar saturation phenomena have been reported in point-source capture systems operating at elevated CO_2 partial pressures (10−20%), suggesting that interfacial saturation is a general feature of catalyst-enhanced gas absorption.[79−82] Importantly, the catalytic enhancement observed at such low concentrations underscores the potency of these biomimetic catalysts and their potential for scalable DAC deployment. The effective concentration of 0.030 mmol is substantially lower than typical loadings used in point-source capture, highlighting the potential for cost-efficient implementation in an industrial-scale DAC process.

Two-Film Theory Analysis and Mass-Transfer Regime

To rigorously assess whether the observed plateau at higher catalyst loadings results from mass-transfer limitations, we performed a comprehensive two-film theory analysis. This analysis calculates the enhancement factor (E) and Hatta number (Ha), which quantifies the relative importance of the chemical reaction versus diffusion in the liquid film. We

Table 2. CO_2 Capture Rate Kinetics with Catalyst ZnC1 and ZnC2 Concentrations in a 1M K_2CO_3 Solution

catalyst concentration (mmol) in 1 M K_2CO_3 solution	capture rate with catalyst ZnC1 (10^{-3} mmol min^{-1}) in 1 M K_2CO_3	enhancement factor E	capture rate with catalyst ZnC2 (10^{-3} mmol min^{-1}) in 1 M K_2CO_3	enhancement factor E
0 mmol (baseline)	0.72	1.00	0.72	1.00
0.008 mmol	0.91	1.26	0.80	1.11
0.015 mmol	1.17	1.63	1.01	1.40
0.030 mmol	1.51	2.10	1.23	1.71
0.045 mmol	1.58	2.19	1.28	1.78
0.080 mmol	1.69	2.35	1.39	1.93

https://doi.org/10.1021/acs.energyfuels.5c06296
Energy Fuels 2026, 40, 5221−5232

calculated the enhancement factor as $E = r/r^0$, where r is the catalytic rate of the reaction and r_0 is the uncatalyzed 1 M K_2CO_3 rate (0 mmol catalyst) as the physical absorption reference ($r_0 = 0.72 \times 10^{-3}$ mmol min^{-1}). E values range from 1.26 to 2.35 for ZnC1 and 1.11 to 1.93 for ZnC2 across different catalyst loadings, demonstrating significant catalytic enhancement with ZnC1 compared to ZnC2 (Table 2, Figure S1 in Supporting Information). The Hatta number quantifies the relative importance of chemical reaction versus diffusion in the liquid film. We calculated it as

$$\mathrm{Ha} = \frac{\sqrt{k_{obs} \times D_{CO2}}}{kL}$$

where k_{obs} represents the observed pseudo-first-order rate constant we calculated from experimental absorption rates, $D_{CO2} = 1.6 \times 10^{-9}$ m^2/s represents the CO_2 diffusivity in carbonate solution at 25 °C, and kL represents the liquid-side mass transfer coefficient. We estimated kL = 5×10^{-5} m/s for our experimental system (an unstirred small reactor with gentle gas sparging producing large bubbles) based on the literature for similar laboratory-scale systems with minimal agitation.[77,83,84] Our calculated Ha values range from 1.45 to 2.22 for ZnC1 and 1.45 to 2.01 for ZnC2 across catalyst loadings (Table 3 and Figures 5 and 6). These values place our system

Table 3. CO_2 Capture Rate Kinetics and Two-Film Theory Analysis with Catalyst ZnC1 and ZnC2 in 1 M K_2CO_3 Solution

catalyst concentration (mmol) in 1 M K_2CO_3 solution	enhancement factor E for ZnC1	Hatta number (Ha) for ZnC1	enhancement factor E for ZnC2	Hatta number (Ha) for ZnC2
0 mmol (baseline)	1.00		1.00	
0.008 mmol	1.26	1.63	1.11	1.53
0.015 mmol	1.63	1.85	1.40	1.71
0.030 mmol	2.10	2.10	1.71	1.90
0.045 mmol	2.19	2.15	1.78	1.93
0.080 mmol	2.35	2.22	1.93	2.01

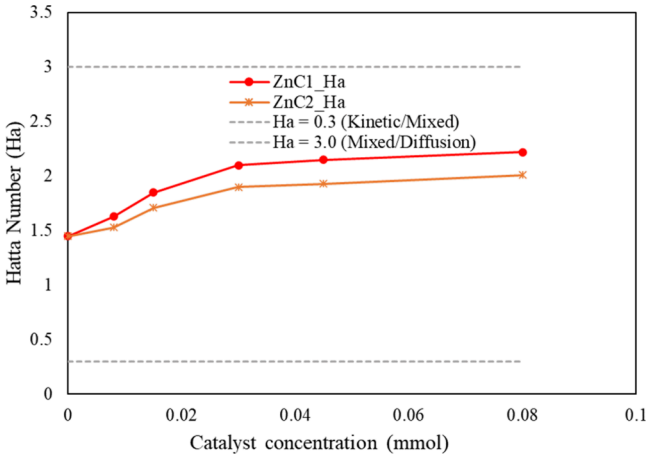

Figure 5. Hatta number versus catalyst concentration showing mixed regime operation. Both ZnC1 and ZnC2 operate in the mixed kinetic/mass-transfer regime (0.3 < Ha < 3).

firmly in the mixed kinetic/mass-transfer regime (0.3 < Ha < 3), where both chemical reaction and physical diffusion contribute comparably to the overall absorption rate. The

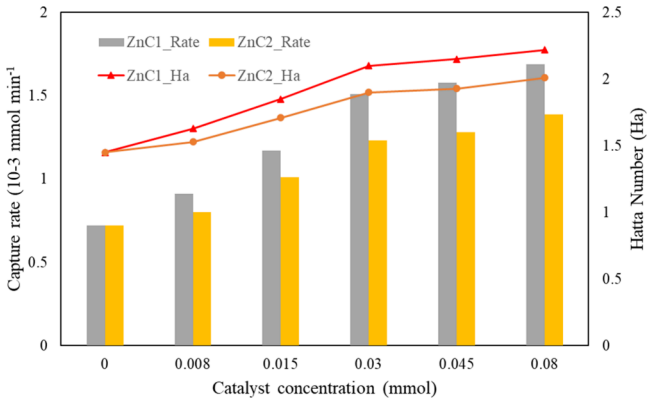

Figure 6. Correlation between CO_2 capture rates and Hatta numbers demonstrating mixed regime operation.

plateau does not result from pure diffusion control (which would require Ha > 3), nor does the system operate under pure kinetic control (Ha < 0.3). Instead, both factors matter, and the system progressively transitions toward more diffusion-influenced conditions as Ha increases to 2.22 (the highest ZnC1 loading).

Foaming Behavior of the ZnC1 and ZnC2 Catalysts

We examined the foaming behavior to understand the influence of gas−bubble interaction on total mass transfer and catalytic efficiency under continuous bubbling conditions relevant to DAC systems.[50,69,70,74] We tested both ZnC1 and ZnC2 in 1 M K_2CO_3 solutions for 30 min with a controlled gas flow rate of 0.5 L/min, measuring the foam height formed over time. ZnC2 produced negligible foam, maintaining a stable foam height below 0.5 cm, while ZnC1 generated slightly higher levels (~2.0 cm), potentially due to differences in ligand geometry and solvation properties (Figure 7). Upon closer

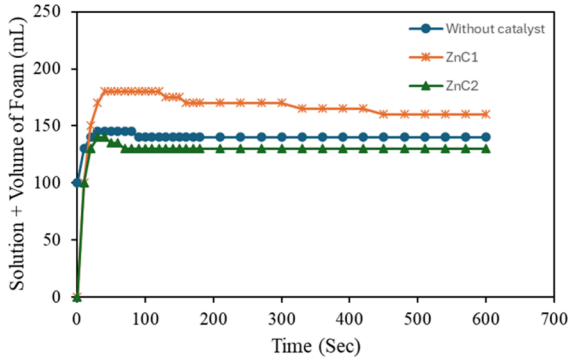

Figure 7. Foaming behaviors of ZnC1 and ZnC2.

inspection, it was clear that foaming in the case without a catalyst and ZnC2 catalyst was solvent displacement due to gas bubbling rather than real foaming. The differential foaming behavior between ZnC1 and ZnC2 (~2 cm vs negligible foam height under identical conditions) is likely due to their structural differences. Single-crystal structure and NMR spectroscopy analyses reveal that the ZnC1 complex has an extended planar geometry with an extended aromatic framework compared to the ZnC2 complex. This structural difference, combined with polar functional groups (Zn center and tertiary amines), gives it a minor amphiphilic character,

https://doi.org/10.1021/acs.energyfuels.5c06296
Energy Fuels 2026, 40, 5221−5232

which may promote interfacial adsorption and foam stabilization.

Our group previously demonstrated this behavior with structurally similar zinc-based carbonic anhydrase mimics.[85] These catalysts accumulate at gas−liquid interfaces, with interfacial concentrations nearly 5-fold higher than in the bulk solution despite minimal changes (<2%) in bulk surface tension. Molecular simulation studies showed that hydrophobic aromatic groups orient toward the gas phase while polar metal centers orient toward the liquid phase, driving this surface accumulation. Importantly, the foaming observed with ZnC1 remains within operationally acceptable limits and does not compromise its superior catalytic performance.

Gas Flow Rate and Capture Efficiency

To evaluate the effect of gas flow rate on CO_2 capture performance,[78] we conducted breakthrough experiments at different flow rates, ranging from 0.1 to 0.5 L/min, with ZnC1 catalyst concentration (0.030 mmol) and sorbent composition (1 M K_2CO_3). As expected, lower flow rates (corresponding to a higher residence time) resulted in better capture efficiency, with the capture rate increasing from 1.5 μmol/min at 0.5 L/min to 4.1 μmol/min at 0.1 L/min (Figure 8). The higher

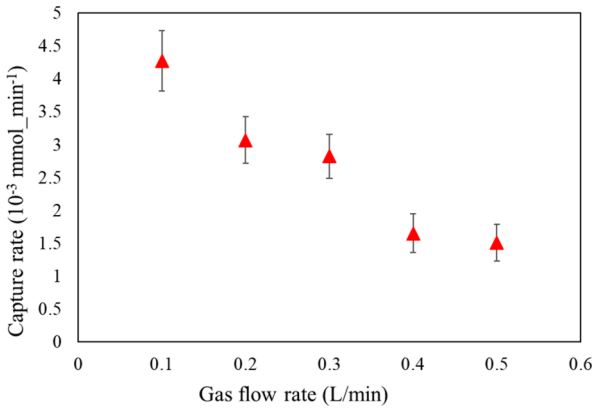

Figure 8. CO_2 capture rate kinetics varying flow rate (L/min) with the ZnC1 catalyst.

residence time at lower flow rates allows higher CO_2−catalyst interaction, thereby improving the overall DAC performance. These findings highlight the critical relationship between the reaction kinetics and the gas flow rate, indicating the necessity for process modification to maximize catalytic efficiency. Also, at a higher gas flow rate, foaming can be worsened, causing liquid carryover and reducing CO_2 absorption efficiency.

Stability of Catalysts

Long-term catalyst stability is a critical requirement for economically viable DAC deployment.[50] To evaluate the stability of ZnC1 and ZnC2 under DAC conditions, we conducted a 24 h continuous capture test in 1 M K_2CO_3 solution. No evidence of catalyst degradation or metal leaching was detected, confirming the structural robustness and chemical compatibility of both complexes in aqueous carbonate media. Postreaction NMR spectra (Figures S20 and S21, Supporting Information) retained characteristic ligand peaks, and UV−vis spectra (Figure S32, Supporting Information) showed no changes in the characteristic ligand-to-metal charge transfer bands (350−450 nm), indicating that the coordination geometry and ligand framework remained intact.

Thermal stability is another important factor for DAC catalysts, particularly in extreme climates. DAC units deployed in hot arid regions may encounter ambient temperatures of 45−50 °C, with solar heating raising internal temperatures to 70−80 °C or higher. To get consistent long-term performance and to prevent catalyst deactivation or unwanted side reactions, it is important to ensure that the catalyst stays stable beyond the DAC operational levels. We carried out thermal stability tests at 150 °C for 6 h in an oven for both catalysts. The postheating capture test confirmed that both catalysts retained more than 95% of their catalytic activity, confirming exceptional thermal stability. UV−vis spectrum (Figure S31, Supporting Information) and ^{1}H NMR spectrum (Figures S16−S19, Supporting Information) measurement confirmed that the catalysts remained intact with no signs of degradation.

Multicycle capture testing is critical for assessing practical viability under continuous DAC operation. However, rigorous cyclability studies require efficient catalyst separation and recovery, which are challenging for these catalysts, where material loss occurs during handling and separation. This proof-of-concept study focuses on establishing the fundamental catalytic activity, structure−activity relationships, and concentration-dependent behavior of Zn-Schiff base complexes under DAC conditions. We are currently developing heterogeneous immobilized versions of these catalysts anchored on solid supports, which will enable a comprehensive cyclability assessment with straightforward separation and recovery.

Solvent Physical Property Impact from Catalysts

To evaluate the true catalytic performance, it is essential to distinguish between genuine catalytic enhancement and that arising through changes in the physical properties of the solution.[50] As the addition of metal complexes to carbonate solutions can modify viscosity, density, and alkalinity, they in turn influence gas−liquid mass transfer coefficients, bubble formation, and interfacial area. Such changes in the physical property can lead to rate enhancement, which is not predictable with catalyst concentration and therefore does not represent true catalysis. In contrast, genuine catalysts accelerate the reaction directly without changing the solution properties, ensuring a consistent performance. To confirm the true catalytic enhancements, we compared the solution alkalinity, viscosity, and density with and without the catalyst (Table 4). We observed no significant changes with viscosity variations below 2% and density changes under 0.5%, both within experimental uncertainty. These negligible changes confirm that the observed rate enhancements of 2.1-fold for

Table 4. Physical Properties of the Solvent in the Presence of ZnC1 and ZnC2 Catalysts

sample	viscosity (cP)	avg viscosity (cP)	density (g/mL)
1 M K_2CO_3	1.40	1.40	1.119
CO_2 loaded 1 M K_2CO_3	1.41	1.41	1.123
fresh ZnC1 in 1 M K_2CO_3	1.4	1.39	1.118
CO_2 loaded ZnC1 solution	1.42	1.42	1.125
fresh ZnC2 in 1 M K_2CO_3	1.37	1.37	1.118
CO_2 loaded ZnC2 solution	1.4	1.39	1.126

https://doi.org/10.1021/acs.energyfuels.5c06296
Energy Fuels 2026, 40, 5221−5232

Scheme 2. Plausible Mechanistic Pathway

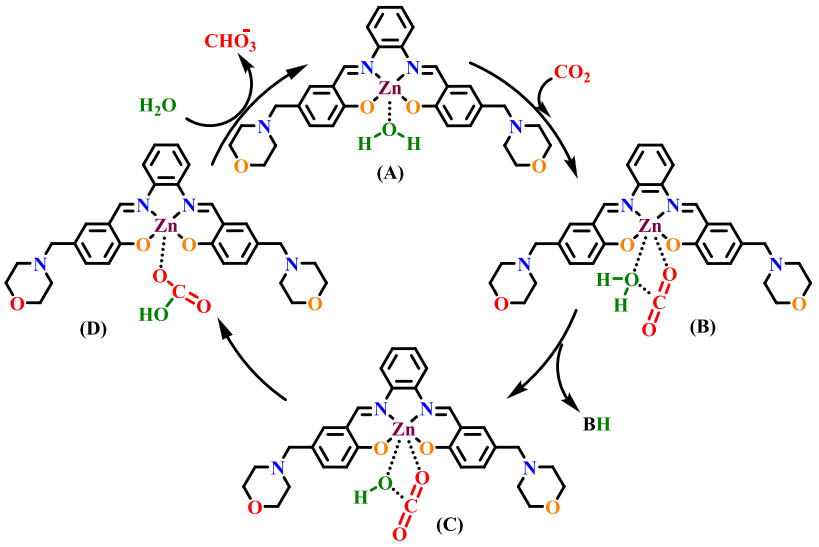

ZnC1 and 1.7-fold for ZnC2 arise from true catalytic enhancement rather than from modifications in the solvent physical properties.

Mechanistic Insights

Both zinc(II) complexes function via a carbonic anhydrase-inspired mechanism,[38−42,45−53,72,73] as illustrated in Scheme 2. The zinc(II) center acts as a Lewis acid that activates water to form a reactive zinc−OH group, which then acts as a nucleophile and attacks CO_2 to start the catalytic conversion into bicarbonate.[4,46,50,52,53] The catalytic cycle begins with binding of water to the four-coordinate zinc(II) center, forming a five-coordinate intermediate. In the basic carbonate environment, this coordinated water undergoes deprotonation to generate a reactive zinc−OH nucleophile that attacks the electrophilic carbon of CO_2. The resulting metal-bicarbonate intermediate undergoes rapid protonation and dissociation to release HCO_3^- and regenerate the active catalyst.

The observed catalytic performance arises from a combination of the structural and electronic features of ZnC1 and ZnC2. The tetradentate salen ligand enforces a planar geometry that facilitates substrate access while mimicking the coordination environment of natural carbonic anhydrase. The phenolic oxygens of the salen ligand act as strong σ-donors, while imine groups contribute to π-back bonding stabilization. The superior activity of ZnC1 over ZnC2 suggests that the resonance stabilization from unsubstituted phenyl rings in ZnC1 dominates the electron-withdrawing effects of the bromo substituent in ZnC2, likely due to enhanced $\pi-\pi$ overlap in the more planar framework. The morpholine-functionalized secondary coordination sphere further enhances catalytic efficiency.[50] The morpholine moiety stabilizes transition states and promotes a favorable substrate orientation through hydrogen bonding. Its weakly basic nitrogen (pK_a ~8.4) can participate in proton relay, facilitating both water deprotonation and bicarbonate release. The conformational flexibility of the six-membered ring allows adaptive reorientation during catalysis, while its polar ether and amine functionalities improve aqueous solubility and suppress aggregation, preserving the effective catalyst concentration. The role of tertiary amines is to facilitate CO_2 uptake by buffering the proton generated during bicarbonate formation, but they do not accelerate the hydration step itself.[38,39,54−56] Tertiary amines promote CO_2 hydration through base-catalyzed proton acceptance, showing first-order dependence on the amine concentration. For industrial flue gas capture, this requires 2.5−5.0 M tertiary amine as the amine functions stoichiometrically as a proton acceptor.[75,76] At our catalyst concentration (0.03 mmol in 25 mL), the free morpholine concentration (~0.6 mmol) is ~1000-fold lower than industrial requirements, insufficient for meaningful base-catalyzed hydration. The observed enhancement originates from the Zn-OH active site, with morpholine serving a secondary-sphere proton-relay role.

The observed enhancement is consistent with the Zn-OH active site mechanism established for carbonic anhydrase mimics, with tertiary amines potentially serving as secondary-sphere proton-transfer groups.[54−56] While we did not perform direct mechanistic studies (e.g., $^{13}CO_2$ labeling, kinetic isotope effects) in this work, the proposed catalytic cycle is supported by (1) the observed rate enhancement and pH profiles, (2) literature precedent for Zn(II)-Schiff base CO_2 hydration catalysts,[4,46,50,72,85] and (3) our recent computational DFT studies mapping the reaction coordinate and identifying Zn-HCO_3^- as a stable intermediate.[50] Direct spectroscopic detection of intermediates via $^{13}CO_2$ labeling and NMR represents a valuable direction for future mechanistic validation. The present catalyst study establishes the fundamental structure−activity relationships and catalytic mechanisms that guide the design of these next-generation immobilized systems for practical large-scale deployment.

CONCLUSIONS

In summary, this work demonstrates that catalyst-assisted direct air capture overcomes the intrinsic kinetic limitations of carbonate-based CO_2 absorption under DAC conditions (~430 ppm of CO_2). Drawing inspiration from carbonic anhydrase, we developed two biomimetic zinc(II) salen complexes, ZnC1 and ZnC2, that promote efficient CO_2 hydration under ambient DAC conditions. ZnC1, in particular, achieves a 2.1× rate enhancement and improves the CO_2 loading capacity at millimolar concentrations, highlighting the impact of molecular design on DAC performance. The catalyst design combines planar salen coordination for electron

https://doi.org/10.1021/acs.energyfuels.5c06296
Energy Fuels 2026, 40, 5221−5232

delocalization, Lewis-acidic Zn(II) center for water activation, and morpholine-functionalized secondary spheres that facilitate proton transfer through hydrogen bonding. The two-film theory analysis reveals that the system operates in the mixed kinetic/mass-transfer regime (1.45 < Ha < 2.22), where both catalyst activity and physical diffusion contribute to the overall performance. The planar geometry of ZnC1 provides higher catalytic efficiency than the sterically distorted ZnC2. This proof-of-concept study establishes Zn-Schiff base complexes as effective biomimetic catalysts for accelerating the hydration of CO_2 under dilute atmospheric conditions. The structure−activity insights provide design principles for next-generation heterogeneous catalyst systems to enable comprehensive cyclability, pH stability, and electrochemical regeneration integration for practical large-scale DAC deployment.

■ ASSOCIATED CONTENT

Supporting Information

The Supporting Information is available free of charge at https://pubs.acs.org/doi/10.1021/acs.energyfuels.5c06296.

Detailed description of materials and methods, including the carbon capture evaluation method and the kinetic rate plot, and two-film theory calculations (including k_{obs} derivation, Ha calculation, and enhancement calculation); compound characterization using ^1H and ^{13}C NMR spectra, high-resolution mass spectra (LC−MS), UV−vis spectra, post-CO_2-capture and post-thermal-treatment ^1H NMR and UV−vis spectra; and associated crystallographic tables/figures (PDF)

Accession Codes

CCDC 2512779 contains the supplementary crystallographic data for this paper.

■ AUTHOR INFORMATION

Corresponding Author

Jesse Thompson − *Institute for Decarbonization and Energy Advancement, University of Kentucky, Lexington, Kentucky 40507, United States; Department of Chemistry, University of Kentucky, Lexington, Kentucky 40506, United States;* orcid.org/0000-0001-7193-4685; Email: jesse.thompson@uky.edu

Authors

Priyabrata Biswal − *Institute for Decarbonization and Energy Advancement, University of Kentucky, Lexington, Kentucky 40507, United States*

Moushumi Sarma − *Institute for Decarbonization and Energy Advancement, University of Kentucky, Lexington, Kentucky 40507, United States;* orcid.org/0000-0003-2134-2387

Xin Gao − *Institute for Decarbonization and Energy Advancement, University of Kentucky, Lexington, Kentucky 40507, United States*

Saloni Bhatnagar − *Institute for Decarbonization and Energy Advancement, University of Kentucky, Lexington, Kentucky 40507, United States*

Sean R. Parkin − *Department of Chemistry, University of Kentucky, Lexington, Kentucky 40506, United States*

Kunlei Liu − *Institute for Decarbonization and Energy Advancement, University of Kentucky, Lexington, Kentucky 40507, United States; Department of Mechanical Engineering, University of Kentucky, Lexington, Kentucky 40506, United States;* orcid.org/0000-0003-3229-0260

Complete contact information is available at: https://pubs.acs.org/10.1021/acs.energyfuels.5c06296

Author Contributions

Priyabrata Biswal, Moushumi Sarma: Conceptualization, Data curation, Writing−original draft, Visualization, Investigation, Formal analysis, Methodology, Validation; Saloni Bhatnagar: Mass spectroscopy analysis; Sean R. Parkin: X-ray crystallography structure analysis; Xin Gao, Kunlei Liu: Supervision, Resources, Project administration, Funding acquisition; Jesse Thompson: Conceptualization, Resources, Supervision, Project administration, Funding acquisition, Review & Editing. The manuscript was written through the contributions of all authors. All authors have given approval to the final version of the manuscript.

Funding

This material is based upon work partially supported by the Department of Energy under award number DE-FE0032255. Support was also received from the PPL Corporation, TotalEnergies, and the Electric Power Research Institute (EPRI).

Notes

The authors declare no competing financial interest.

■ ABBREVIATIONS

DAC,direct air capture; CO_2,carbon dioxide

■ REFERENCES

(1) Masson-Delmotte, V.; Zhai, P.; Pirani, A.; Connors, S. L.; Péan, C.; Berger, S.; Caud, N.; Chen, Y.; Goldfarb, L.; Gomis, M. Climate change 2021: the physical science basis. *Contribution of working group I to the sixth assessment report of the intergovernmental panel on climate change* **2021**, *2* (1), 2391.

(2) Bongaarts, J., IPCC, 2023: Climate Change 2023: Synthesis Report. IPCC, 184 p., doi: . Wiley Online Library: 2024.

(3) Jain, A. K. Global carbon budget 2022. *Earth Syst. Sci. Data* **2022**, *14* (11), 4811−4900.

(4) Lippert, C. A.; Liu, K.; Sarma, M.; Parkin, S. R.; Remias, J. E.; Brandewie, C. M.; Odom, S. A.; Liu, K. Improving carbon capture from power plant emissions with zinc-and cobalt-based catalysts. *Catal. Sci. Technol.* **2014**, *4* (10), 3620−3625.

(5) Intergovernmental Panel on Climate, C. *Global Warming of 1.5°C: IPCC Special Report on Impacts of Global Warming of 1.5°C above Pre-industrial Levels in Context of Strengthening Response to Climate Change, Sustainable Development, and Efforts to Eradicate Poverty*. Cambridge University Press, 2022. DOI: .

(6) Jeswani, H. K.; Azapagic, A.; Saharudin, D. M. Environmental sustainability of negative emissions technologies: A review. *Sustain. Prod. Consum.* **2022**, *33*, 608−635.

(7) Markusson, N.; McLaren, D.; Tyfield, D. Towards a cultural political economy of mitigation deterrence by negative emissions technologies (NETs). *Glob. Sustain.* **2018**, *1*, No. e10.

(8) Chuah, C. Y.; Ho, Y. L.; Syed, A. M. H.; Thivyalakshmi, K. G. K.; Yang, E.; Johari, K.; Yang, Y.; Poon, W. C. Applicability of adsorbents in direct air capture (DAC): Recent progress and future perspectives. *Ind. Eng. Chem. Res.* **2025**, *64* (8), 4117−4147.

(9) Erans, M.; Sanz-Pérez, E. S.; Hanak, D. P.; Clulow, Z.; Reiner, D. M.; Mutch, G. A. Direct air capture: process technology, techno-economic and socio-political challenges. *Energy Environ. Sci.* **2022**, *15* (4), 1360−1405.

(10) Wang, J.; Feng, X.; Wen, S.; Zhan, D.; Zhu, X.; Ning, P.; Zhang, Y.; Mei, X. Recent advances in amine-functionalized silica adsorbents for CO_2 capture. *Renew. Sustain. Energy Rev.* **2024**, *203*, No. 114724.
(11) Zhu, X.; Xie, W.; Wu, J.; Miao, Y.; Xiang, C.; Chen, C.; Ge, B.; Gan, Z.; Yang, F.; Zhang, M.; et al. Recent advances in direct air capture by adsorption. *Chem. Soc. Rev.* **2022**, *51* (15), 6574−6651.
(12) Chang, S.-F.; Chiu, H.-H.; Jao, H.-S.; Shang, J.; Lin, Y.-J.; Yu, B.-Y. Comprehensive evaluation of various CO_2 capture technologies through rigorous simulation: Economic, equipment footprint, and environmental analysis. *Carbon Capture Sci. Technol.* **2025**, *14*, No. 100342.
(13) Dhingra, G.; Kumar, A. Carbon Capture and Sequestration: Cutting-Edge Technologies to Combat Climate Change. *Sustain. Energy Technol. Assess.* **2025**, *75*, No. 104226.
(14) Jiang, Y.; Mathias, P. M.; Zheng, R. F.; Freeman, C. J.; Barpaga, D.; Malhotra, D.; Koech, P. K.; Zwoster, A.; Heldebrant, D. J. Energy-effective and low-cost carbon capture from point-sources enabled by water-lean solvents. *J. Clean. Prod.* **2023**, *388*, No. 135696.
(15) Ozden, A.; Luo, M.; Lum, Y. Point-source carbon capture and direct air capture−A technology overview. *Chem. Eng. J.* **2025**, *519*, No. 165535.
(16) Zanobetti, F.; Dal Pozzo, A.; Cozzani, V. Sustainability assessment of CO_2 capture across different scales of hard-to-abate emission sources. *Chem. Eng. J.* **2025**, *505*, No. 159466.
(17) Fuss, S.; Lamb, W. F.; Callaghan, M. W.; Hilaire, J.; Creutzig, F.; Amann, T.; Beringer, T.; de Oliveira Garcia, W.; Hartmann, J.; Khanna, T.; Luderer, G.; Nemet, G. F.; Rogelj, J.; Smith, P.; Vicente, J. L. V.; Wilcox, J.; del Mar Zamora Dominguez, M.; Minx, J. C. Negative emissions—Part 2: Costs, potentials and side effects. *Environ. Res. Lett.* **2018**, *13* (6), No. 063002.
(18) IEA. Direct air capture: A key technology for net zero. *OECD***2022**.
(19) Keith, D. W.; Holmes, G.; St. Angelo, D.; Heidel, K. A process for capturing CO_2 from the atmosphere. *Joule* **2018**, *2* (8), 1573−1594.
(20) Sabatino, F.; Grimm, A.; Gallucci, F.; van Sint Annaland, M.; Kramer, G. J.; Gazzani, M. A comparative energy and costs assessment and optimization for direct air capture technologies. *Joule* **2021**, *5* (8), 2047−2076.
(21) Sodiq, A.; Abdullatif, Y.; Aissa, B.; Ostovar, A.; Nassar, N.; El-Naas, M.; Amhamed, A. A review on progress made in direct air capture of CO_2. *Environ. Technol. Innov.* **2023**, *29*, No. 102991.
(22) Ozkan, M.; Nayak, S. P.; Ruiz, A. D.; Jiang, W. Current status and pillars of direct air capture technologies. *Iscience* **2022**, *25* (4), No. 103990.
(23) Goswami, N.; Rao, S.; Abad, S. D.; Ruba, A.; Thakkar, H.; Mukherjee, P. P.; Singh, R. P.; Spendelow, J. S.; Holby, E. F.; Zelenay, P.; et al. Role of Hierarchical Porosity in Dictating Adsorption Dynamics in Direct Air Capture Systems. *ACS Appl. Energy Mater.* **2025**, *8* (15), 11758−11770.
(24) Kotowicz, J.; Niesporek, K.; Baszczeńska, O. Advancements and Challenges in Direct Air Capture Technologies: Energy Intensity, Novel Methods, Economics, and Location Strategies. *Energies* **2025**, *18* (3), 496.
(25) Liu, H.; Lin, H.; Dai, S.; Jiang, D.-e. Minimal Kinetic Model of Direct Air Capture of CO_2 by Supported Amine Sorbents in Dry and Humid Conditions. *Ind. Eng. Chem. Res.* **2024**, *63* (13), 5871−5879.
(26) de Jonge, M. M.; Daemen, J.; Loriaux, J. M.; Steinmann, Z. J.; Huijbregts, M. A. Life cycle carbon efficiency of Direct Air Capture systems with strong hydroxide sorbents. *Int. J. Greenh. Gas Control.* **2019**, *80*, 25−31.
(27) Ghaffari, S.; Gutierrez, M. F.; Seidel-Morgenstern, A.; Lorenz, H.; Schulze, P. Sodium hydroxide-based CO_2 direct air capture for soda ash production— fundamentals for process engineering. *Ind. Eng. Chem. Res.* **2023**, *62* (19), 7566−7579.
(28) Holmes, G.; Keith, D. W. An air−liquid contactor for large-scale capture of CO_2 from air. *Philosophical Transactions of the Royal Society A: Mathematical, Physical and Engineering Sciences* **2012**, *370* (1974), 4380−4403.
(29) Stolaroff, J. K.; Keith, D. W.; Lowry, G. V. Carbon dioxide capture from atmospheric air using sodium hydroxide spray. *Environ. Sci. Technol.* **2008**, *42* (8), 2728−2735.
(30) Zahedi, R.; Ayazi, M.; Aslani, A. Comparison of amine adsorbents and strong hydroxides soluble for direct air CO_2 capture by life cycle assessment method. *Environ. Technol. Innov.* **2022**, *28*, No. 102854.
(31) Shi, X.; Xiao, H.; Azarabadi, H.; Song, J.; Wu, X.; Chen, X.; Lackner, K. S. Sorbents for the direct capture of CO_2 from ambient air. *Angew. Chem., Int. Ed.* **2020**, *59* (18), 6984−7006.
(32) Wurzbacher, J. A.; Gebald, C.; Piatkowski, N.; Steinfeld, A. Concurrent separation of CO_2 and H_2O from air by a temperature-vacuum swing adsorption/desorption cycle. *Environ. Sci. Technol.* **2012**, *46* (16), 9191−9198.
(33) Fasihi, M.; Efimova, O.; Breyer, C. Techno-economic assessment of CO_2 direct air capture plants. *J. Clean. Prod.* **2019**, *224*, 957−980.
(34) McQueen, N.; Gomes, K. V.; McCormick, C.; Blumanthal, K.; Pisciotta, M.; Wilcox, J. A review of direct air capture (DAC): scaling up commercial technologies and innovating for the future. *Prog. Energy.* **2021**, *3* (3), No. 032001.
(35) National Academies of Sciences, Medicine, Division on Earth, Life Studies, Ocean Studies Board, Board on Chemical Sciences, Board on Earth Sciences, Board on Energy, Environmental Systems, Board on Atmospheric Sciences and Committee on Developing a Research Agenda for Carbon Dioxide Removal, 2019. *Negative emissions technologies and reliable sequestration*; A research agenda. 2019.
(36) Kasturi, A.; Gug Jang, G.; Stamberga, D.; Custelcean, R.; Yiacoumi, S.; Tsouris, C. Determination of the regeneration energy of direct air capture solvents/sorbents using calorimetric methods. *Sep. Purif. Technol.* **2023**, *310*, No. 123154.
(37) Realmonte, G.; Drouet, L.; Gambhir, A.; Glynn, J.; Hawkes, A.; Köberle, A. C.; Tavoni, M. An inter-model assessment of the role of direct air capture in deep mitigation pathways. *Nat. Commun.* **2019**, *10* (1), 3277.
(38) Lindskog, S. Structure and mechanism of carbonic anhydrase. *Pharmacol. Ther.* **1997**, *74* (1), 1−20.
(39) Silverman, D. N.; Lindskog, S. The catalytic mechanism of carbonic anhydrase: implications of a rate-limiting protolysis of water. *Acc. Chem. Res.* **1988**, *21* (1), 30−36.
(40) Christianson, D. W.; Fierke, C. A. Carbonic anhydrase: evolution of the zinc binding site by nature and by design. *Acc. Chem. Res.* **1996**, *29* (7), 331−339.
(41) Supuran, C. T. Structure and function of carbonic anhydrases. *Biochem. J.* **2016**, *473* (14), 2023−2032.
(42) Floyd, W. C., III; Baker, S. E.; Valdez, C. A.; Stolaroff, J. K.; Bearinger, J. P.; Satcher, J. H., Jr.; Aines, R. D. Evaluation of a carbonic anhydrase mimic for industrial carbon capture. *Environ. Sci. Technol.* **2013**, *47* (17), 10049−10055.
(43) Floyd, W. C.; Baker, S. E.; Valdez, C. A.; Stolaroff, J. K.; Bearinger, J. P.; Satcher, J. H.; Aines, R. D. Evaluation of a Carbonic Anhydrase Mimic for Industrial Carbon Capture. *Environ. Sci. Technol.* **2013**, *47* (17), 10049−10055.
(44) Huang, D.; Makhlynets, O. V.; Tan, L. L.; Lee, S. C.; Rybak-Akimova, E. V.; Holm, R. H. Fast Carbon Dioxide Fixation by 2,6-Pyridinedicarboxamidato-nickel(II)-hydroxide Complexes: Influence of Changes in Reactive Site Environment on Reaction Rates. *Inorg. Chem.* **2011**, *50* (20), 10070−10081.
(45) Kelsey, R. A.; Miller, D. A.; Parkin, S. R.; Liu, K.; Remias, J. E.; Yang, Y.; Lightstone, F. C.; Liu, K.; Lippert, C. A.; Odom, S. A. Carbonic anhydrase mimics for enhanced CO_2 absorption in an amine-based capture solvent. *Dalton Trans.* **2016**, *45* (1), 324−333.
(46) Koziol, L.; Valdez, C. A.; Baker, S. E.; Lau, E. Y.; Floyd, W. C.; Wong, S. E.; Satcher, J. H.; Lightstone, F. C.; Aines, R. D. Toward a small molecule, biomimetic carbonic anhydrase model: theoretical and experimental investigations of a panel of zinc (II) aza-macrocyclic catalysts. *Inorg. Chem.* **2012**, *51* (12), 6803−6812.

https://doi.org/10.1021/acs.energyfuels.5c06296
Energy Fuels 2026, 40, 5221−5232

(47) Liang, S.; Wu, X.-L.; Zong, M.-H.; Lou, W.-Y. Zn-triazole coordination polymers: Bioinspired carbonic anhydrase mimics for hydration and sequestration of CO_2. *Chem. Eng. J.* **2020**, *398*, No. 125530.
(48) Nakata, K.; Shimomura, N.; Shiina, N.; Izumi, M.; Ichikawa, K.; Shiro, M. Kinetic study of catalytic CO_2 hydration by water-soluble model compound of carbonic anhydrase and anion inhibition effect on CO_2 hydration. *J. Inorg. Biochem.* **2002**, *89* (3−4), 255−266.
(49) Sahoo, P. C.; Jang, Y.-N.; Lee, S.-W. Immobilization of carbonic anhydrase and an artificial Zn (II) complex on a magnetic support for biomimetic carbon dioxide sequestration. *J. Mol. Catal. B Enzym.* **2012**, *82*, 37−45.
(50) Widger, L. R.; Sarma, M.; Kelsey, R. A.; Risko, C.; Lippert, C. A.; Parkin, S. R.; Liu, K. Enhancing CO_2 absorption for post-combustion carbon capture via zinc-based biomimetic catalysts in industrially relevant amine solutions. *Int. J. Greenh. Gas Control.* **2019**, *85*, 156−165.
(51) Yong, J. K.; Stevens, G. W.; Caruso, F.; Kentish, S. E. The use of carbonic anhydrase to accelerate carbon dioxide capture processes. *J. Chem. Technol. Biotechnol.* **2015**, *90* (1), 3−10.
(52) Zhang, X.; van Eldik, R. A functional model for carbonic anhydrase: thermodynamic and kinetic study of a tetraazacyclododecane complex of zinc (II). *Inorg. Chem.* **1995**, *34* (22), 5606−5614.
(53) Zhang, X.; van Eldik, R.; Koike, T.; Kimura, E. Kinetics and mechanism of the hydration of carbon dioxide and dehydration of bicarbonate catalyzed by a zinc (II) complex of 1, 5, 9-triazacyclododecane as a model for carbonic anhydrase. *Inorg. Chem.* **1993**, *32* (25), 5749−5755.
(54) Briš, A.; Margetić, D. Hydrogen-Bonding Secondary Coordination Sphere Effect on CO_2 Reduction. *Organics* **2023**, *4* (2), 277−288.
(55) Mann, S. I.; Heinisch, T.; Ward, T. R.; Borovik, A. S. Coordination chemistry within a protein host: regulation of the secondary coordination sphere. *Chem. Commun.* **2018**, *54* (35), 4413−4416.
(56) Shook, R. L.; Borovik, A. Role of the secondary coordination sphere in metal-mediated dioxygen activation. *Inorg. Chem.* **2010**, *49* (8), 3646−3660.
(57) Lu, G.; Farrukh, S.; Fan, X. Research progress of non-aqueous absorbents for carbon dioxide capture with low energy consumption: A review. *Fuel.* **2025**, *391*, No. 134740.
(58) Nokpho, P.; Amornsin, P.-o.; Boonmatoon, P.; Wang, X.; Chalermsinsuwan, B. Evaluating regeneration performance of amine functionalized solid sorbents for direct air CO_2 capture using microwave. *Mater. Today Sustain.* **2024**, *26*, No. 100728.
(59) Rochelle, G. T. Amine scrubbing for CO_2 capture. *Science* **2009**, *325* (5948), 1652−1654.
(60) Spigarelli, B. P.; Kawatra, S. K. Opportunities and challenges in carbon dioxide capture. *J. CO_2 Util.* **2013**, *1*, 69−87.
(61) Waseem, M.; Al-Marzouqi, M.; Ghasem, N. A review of catalytically enhanced CO_2-rich amine solutions regeneration. *J. Environ. Chem. Eng.* **2023**, *11* (4), No. 110188.
(62) Zhang, X.; Fang, Z.; Zhu, P.; Xia, Y.; Wang, H. Electrochemical regeneration of high-purity CO_2 from (bi)carbonates in a porous solid electrolyte reactor for efficient carbon capture. *Nat. Energy* **2025**, *10* (1), 55−65.
(63) Ohiomoba, E.; Omosebi, A.; Kharel, P.; Gao, X.; Liu, K. Electrochemical stripping of CO_2 from potassium-based salts to facilitate direct air capture. *Electrochim. Acta* **2025**, *512*, No. 145521.
(64) Keith, D. W. Why capture CO_2 from the atmosphere? *Science* **2009**, *325* (5948), 1654−1655.
(65) Mahmoudkhani, M.; Keith, D. W. Low-energy sodium hydroxide recovery for CO_2 capture from atmospheric air—Thermodynamic analysis. *Int. J. Greenh. Gas Control* **2009**, *3* (4), 376−384.
(66) Mantripragada, H. C.; Rubin, E. S. Calcium looping cycle for CO_2 capture: Performance, cost and feasibility analysis. *Energy Procedi* **2014**, *63*, 2199−2206.
(67) Ozcan, D. C.; Alonso, M.; Ahn, H.; Abanades, J. C.; Brandani, S. Process and cost analysis of a biomass power plant with in situ calcium looping CO_2 capture process. *Ind. Eng. Chem. Res.* **2014**, *53* (26), 10721−10733.
(68) Øi, L. E.*Aspen HYSYS simulation of CO_2 removal by amine absorption from a gas based power plant. In The 48th Scandinavian Conference on Simulation and Modeling (SIMS 2007)*, 2007; Linköping University Electronic Press: Göteborg (Särö), pp 30−31.
(69) Thitakamol, B.; Veawab, A.; Aroonwilas, A. Foaming in amine-based CO_2 capture process: experiment, modeling and simulation. *Energy Procedia* **2009**, *1* (1), 1381−1386.
(70) Tiwari, S. P.; Steckel, J. A.; Sarma, M.; Bryant, J.; Lippert, C. A.; Widger, L. R.; Thompson, J.; Liu, K.; Siefert, N.; Hopkinson, D.; et al. Foaming Dependence on the Interface Affinities of Surfactant-like Molecules. *Ind. Eng. Chem. Res.* **2019**, *58* (43), 19877−19889.
(71) Liu, K.; Frimpong, R.; Landon, J.; Lippert, C.; Richburg, L.; Thompson, J.; Vaysman, V.; Mace, E.; Whitney, C. *Research Foundation*; Univ. of Kentucky: Lexington, KY (United States **2017**.
(72) Widger, L. R.; Sarma, M.; Bryant, J. J.; Mannel, D. S.; Thompson, J. G.; Lippert, C. A.; Liu, K. Enhancements in mass transfer for carbon capture solvents part I: Homogeneous catalyst. *Int. J. Greenh. Gas Control* **2017**, *63*, 249−259.
(73) Bond, G. M.; Stringer, J.; Brandvold, D. K.; Simsek, F. A.; Medina, M.-G.; Egeland, G. Development of integrated system for biomimetic CO_2 sequestration using the enzyme carbonic anhydrase. *Energy Fuels* **2001**, *15* (2), 309−316.
(74) Thitakamol, B.; Veawab, A. Foaming Behavior in CO_2 Absorption Process Using Aqueous Solutions of Single and Blended Alkanolamines. *Ind. Eng. Chem. Res.* **2008**, *47* (1), 216−225.
(75) Kopitha, K.; Elakneswaran, Y.; Kitagaki, R.; Saito, R.; Tsujino, M.; Nishida, A.; Senboku, H.; Hiroyoshi, N. N-methyldiethanolamine (MDEA) as an effective CO_2 absorbent for direct air capture (DAC) in cement-based materials. *Chem. Eng. J.* **2023**, *475*, No. 146067.
(76) Li, G.; Shen, X.; Jiao, X.; Xie, F.; Hua, J.; Lin, H.; Yan, F.; Wu, H.; Zhang, Z. Novel tri-solvent amines absorption for flue gas CO_2 capture: Efficient absorption and regeneration with low energy consumption. *Chem. Eng. J.* **2024**, *493*, No. 152699.
(77) Mannel, D. S.; Qi, G.; Widger, L. R.; Bryant, J.; Liu, K.; Fegenbush, A.; Lippert, C. A.; Liu, K. Enhancements in mass transfer for carbon capture solvents part II: Micron-sized solid particles. *Int. J. Greenh. Gas Control* **2017**, *61*, 138−145.
(78) Zaghini, A.; Badino, S. F.; Neun, S.; Westh, P. Enzyme assisted direct air capture of carbon dioxide. *Carbon Capture Sci. Technol.* **2025**, *14*, No. 100369.
(79) Alper, E.; Deckwer, W.-D. Kinetics of absorption of CO_2 into buffer solutions containing carbonic anhydrase. *Chem. Eng. Sci.* **1980**, *35* (3), 549−557.
(80) Du, Y.; Wang, Y.; Rochelle, G. T. Piperazine/4-hydroxy-1-methylpiperidine for CO_2 capture. *Chem. Eng. J.* **2017**, *307*, 258−263.
(81) Penders-van Elk, N. J.; Hamborg, E. S.; Huttenhuis, P. J.; Fradette, S.; Carley, J. A.; Versteeg, G. F. Kinetics of absorption of carbon dioxide in aqueous amine and carbonate solutions with carbonic anhydrase. *Int. J. Greenh. Gas Control.* **2013**, *12*, 259−268.
(82) Ye, X.; Lu, Y. CO_2 absorption into catalyzed potassium carbonate−bicarbonate solutions: Kinetics and stability of the enzyme carbonic anhydrase as a biocatalyst. *Chem. Eng. Sci.* **2014**, *116*, 567−575.
(83) Bishnoi, S.; Rochelle, G. T. Absorption of carbon dioxide into aqueous piperazine: reaction kinetics, mass transfer and solubility. *Chem. Eng. Sci.* **2000**, *55* (22), 5531−5543.
(84) Dugas, R.; Rochelle, G. Absorption and desorption rates of carbon dioxide with monoethanolamine and piperazine. *Energy Procedia* **2009**, *1* (1), 1163−1169.
(85) Shi, W.; Widger, L. R.; Sarma, M.; Lippert, C. A.; Alman, D. E.; Liu, K. Molecular Modeling of the Physical Properties for Aqueous Amine Solution Containing a CO_2 Hydration Catalyst. *Ind. Eng. Chem. Res.* **2017**, *56* (40), 11644−11651.

https://doi.org/10.1021/acs.energyfuels.5c06296
Energy Fuels 2026, 40, 5221−5232